NUCL SCI TECH (2017) 28:101
DOI 10.1007/s41365-017-0256-1

Energy response correction for an electronic personal dosimeter using the channel ratio method

Ping Huang[1,2] · You-De Zhang[1] · Yong Yang[1,2] · Cong-Hua Zhang[1,3] · Lan Gong[1,2] · Qian Yang[1,3]

Received: 17 February 2017 / Revised: 16 May 2017 / Accepted: 18 May 2017 / Published online: 7 June 2017

Abstract An electronic personal dosimeter mainly uses a Si-PIN photodiode as X- and gamma-ray detectors. The photon energy response of this instrument is inconsistent in the case of no correction, which seriously affects the accurate monitoring of personal dose equivalent $H_p(10)$ parameters for radiation workers. For this reason, in this paper we propose a method of combining composite screen detection technology, multichannel measurement technology, and the channel ratio method to achieve accurate measurement of the personal dose equivalent parameters. According to China National Standard GB/T 13161-2003 and National Verification Regulation JJG 1009-2006, the instrument was tested in the energy range between 48 keV and 1.25 MeV. The experimental results showed that the difference of energy response to $^{137}C_s$ corrected by the new method was almost constant within ±6.0%, which fulfilled the ±30% requirement of GB/T 13161-2003 and JJG 1009-2006. Meanwhile, the method proposed obtained energy information regarding the radiation field.

This work was supported by the National Key Scientific Instruments To Develop Dedicated (2013YQ090811).

✉ Ping Huang
zhangyaohp@163.com

1 National Institute of Measurement and Testing Technology, Chengdu 610021, China

2 Sichuan Radiation Technology Co., Ltd., Chengdu 610021, China

3 Nimtt Measurement and Testing Technology, Ltd, Chengdu 610021, China

Keywords Electronic personal dosimeter (EPD) · Si-PIN detector · Photon energy response · Channel ratio method (CRM)

1 Introduction

The electronic personal dosimeter (EPD), characterized by miniaturization, multi-functionality, wide measuring range, real-time measurement, and low power consumption, has been widely used in personal dose equivalent $H_p(10)$ monitoring in nuclear power environments, nuclear reactors, nuclear medicine, and other workplaces in which humans are exposed to radiation [1–3]. Since the Si-PIN semiconductor detector has advantages in sensitivity, volume, power consumption, price, etc., it is one of the key components of the EPD system [4–6]. At the same time, the Si-PIN detector has difficulty forming the equilibrium condition of charged particles because the atomic coefficient of the detector is higher than that of the tissue material and the sensitive layer is thin. For these reasons, the photon energy response of a Si-PIN detector is not consistent in the energy range from 48 keV to 1.25 MeV, especially in the low-energy region (less than 100 keV), where the photon energy response to $^{137}C_s$ is high.

Because the energy response of a Si-PIN detector is not consistent, using the traditional single-channel counting method seriously affects the measurement accuracy of the instrument, so it is necessary to solve this problem by other methods. The method of correcting the energy response of a Si-PIN detector is one of the core technologies of an EPD. EPDs based on a Si-PIN detector mainly include three kinds of methods for energy response correction, namely the compensation material method, the spectrometer–dosimeter method, and the channel ratio method (CRM).

The related parameters of an energy-compensated material can be calculated by numerical calculation or Monte Carlo simulation [7–10]. The core idea of this method is to design a kind of composite material that can achieve the purpose of off-setting the high response of the Si-PIN detector in the low-energy region [11–14]. The difficulty of this method resides in its inability to process bulk materials to meet performance requirements. At the same time, the measurement error of this method is correspondingly large, and the performance requirements of a Si-PIN detector are relatively high.

The spectrometer–dosimeter method measures the pulse-height spectra of the Si-PIN detector, and the linear relationship between the pulse amplitude and the absorbed energy at the Si-PIN detector is obtained by experiments [15, 16]. Because the influence of photons of different energies on the personal dose equivalent ($H_p(10)$) is different, the energy response correction of the Si-PIN detector can be realized by using the counts of each channel multiplied by weighting factors [17]. However, this method does not meet the basic requirements of the EPD because of its power consumption, size, cost, and other factors. Historically, some authors have put forward a simplified multichannel spectrometric system by using a few comparators, and the energy response correction of the detector was done in the same way. This method can reduce the power consumption and the cost of the instrument, but it is difficult to adjust the threshold parameters, and the measurement accuracy is limited. Another method was called the dose conversion unit (DCU), which considered the pulse amplitude as well as the pulse number simultaneously. The DCU used a microprocessor to control a digital-to-analog converter (DAC), and the output of the DAC was fed into a single-channel analyzer (SCA) as low-level discriminator (LLD) values based on the dose conversion function. The final output of the DCU system was the count rates of pulses, which were directly proportional to the exposure dose rate in air [18, 19]. From the relevant literature [17–19], it was found that this method had some limitations in the measuring range; in addition, the system structure and the calculation methods were relatively complex.

The basic idea of the CRM is that there is a relationship between the channel ratio value and the beam energy. By changing the thickness of the additional filter material of the two channels, the beam energy can be identified using the CRM. By utilizing the conversion factor under the specific energy conditions, the personal dose equivalent parameters can be obtained. So far, the CRM has not been successfully applied in the EPD, but the method has potential application value in neutron-gamma resolution and beta measurements [20–22].

In summary, the CRM is more advantageous in terms of instrument structure than the spectrometer–dosimeter method, and its measurement accuracy is higher than the compensation material method. Therefore, in this paper we focus on the principle and method of using the CRM to correct the photon energy response of an EPD.

2 Mathematical relationship between channel ratio and beam energy

Figure 1 is a schematic of the two-channel ratio method. CM_1 and CM_2 are composite filter materials, the thicknesses are T_1 (cm) and T_2 (cm), the linear attenuation coefficients are $\mu_1(E)$ (cm^{-1}) and $\mu_2(E)$ (cm^{-1}), and the sensitive area is S (cm^2). D_1 and D_2 are the Si-PIN detectors, the thickness of the sensitive layer is T_3 (cm), the linear attenuation coefficient is $\mu_3(E)$ (cm^{-1}), and the sensitive area is S (cm^2). Channel 1 (CH_1) consists of a composite material CM_1 and a Si-PIN detector D_1; channel 2 (CH_2) consists of a composite material CM_2 and a Si-PIN detector D_2.

The back end of each channel also includes a charge-sensitive amplifier, a main amplifier, and a discriminator circuit (shown in Fig. 2). The multichannel design method is based on the extension of the measuring range, and the correction principle of the small detector is the same as that of the large detector.

Assuming that the particle fluence at the detector position is D_S (cm^{-2}), the particle energy is E (keV), and the particle numbers interacting with the Si-PIN detector are DM_1 and DM_2. Assuming that particles interacting with the Si-PIN detector are recorded by the subsequent circuit, the following relationship exists:

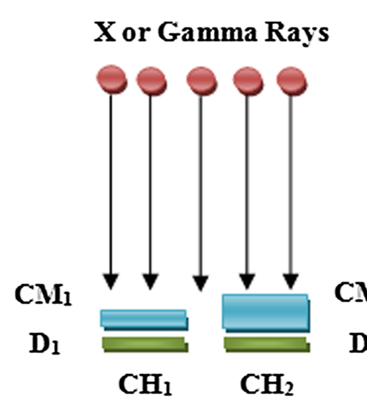

Fig. 1 (Color online) Schematic of the measurement principle of the two-channel ratio method

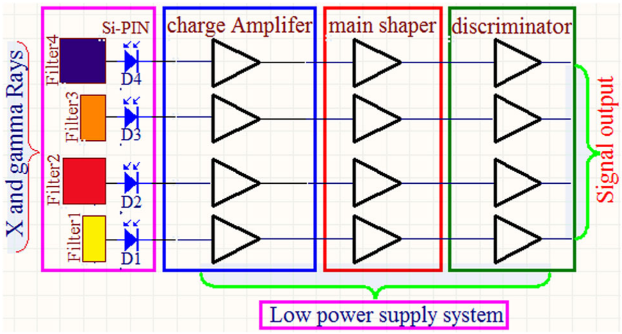

Fig. 2 (Color online) Schematic of the multichannel measurement

$$\begin{cases} \mathrm{DM}_1 = D_s e^{-\mu_1(E)T_1}(1 - e^{-\mu_3(E)T_3})S, \\ \mathrm{DM}_2 = D_s e^{-\mu_2(E)T_2}(1 - e^{-\mu_3(E)T_3})S. \end{cases} \tag{1}$$

When $\mu_1(E)$ is equal to $\mu_2(E)$, Eq. (1) is further simplified as follows:

$$\mu_1(E) = \ln(\mathrm{DM}_1/\mathrm{DM}_2)/(T_2 - T_1). \tag{2}$$

The linear attenuation coefficient $\mu_1(E)$ can be calculated using Eq. (2). If the corresponding relation between $\mu_1(E)$ and E is successfully established in a table, the energy information of the radiation field is obtained using the look-up table (LUT) method. Meanwhile, the channel ratio value and the beam energy should have a one-to-one relationship in the measurement range. $\mu_1(E)$ should satisfy the monotone function characteristic in the energy range from 48 keV to 1.25 MeV. When the physical form of the filter material is considered, the photon mass attenuation coefficient $[\mu_1(E)/\rho]$ is often used to describe the reduction in the photon fluence , where ρ is the density of the composite filter material (g/cm^3) [23, 24]. After utilizing the mass attenuation coefficient, the basic feature remains unchanged.

The calculation model under the monotone energy radiation field is now discussed. In the continuous spectrum of the radiation field (such as the X-ray diagnostic radiation source), Eq. (2) will be complex, and is transformed to

$$\begin{cases} \mathrm{DM}_1 = [\phi(E_1)e^{-\mu_1(E_1)T_1}(1 - e^{-\mu_3(E_1)T_3}) \\ \qquad + \phi(E_2)e^{-\mu_1(E_2)T_1}(1 - e^{-\mu_3(E_2)T_3}) \\ \qquad + \ldots + \phi(E_n)e^{-\mu_1(E_n)T_1}(1 - e^{-\mu_3(E_n)T_3})]S, \\ \mathrm{DM}_2 = [\phi(E_1)e^{-\mu_1(E_1)T_2}(1 - e^{-\mu_3(E_1)T_3}) \\ \qquad + \phi(E_2)e^{-\mu_1(E_2)T_2}(1 - e^{-\mu_3(E_2)T_3}) \\ \qquad + \ldots + \phi(E_n)e^{-\mu_1(E_n)T_2}(1 - e^{-\mu_3(E_n)T_3})]S, \end{cases} \tag{3}$$

where $\phi(E_1)$, $\phi(E_2)$, ... , $\phi(E_n)$ are the particle fluences (cm^{-2}), $E_1, E_2, \ldots, E_n$ are the energy of the X-ray particles (keV), and n indicates the particles of different energy. Although DM_1, DM_2, and the thickness of the composite material are known, the value $\mu_1(E)$ is difficult to obtain using Eq. (3).

Equations (1)–(3) are established on the premise that the detection system meets the narrow-beam geometry. Under broad-beam geometry (BBG) conditions, the influence of the scattered photons must be considered, and the $\mu_1(E)$ value of the filter material is not accurately computed using the channel ratio value. Owing to the EPD having performance requirements for angle response and sensitivity, the detector unit is in the BBG condition, assuming that the scattered photons are recorded by the subsequent circuit under the BBG condition. When using the buildup factor to correct the scattered photons, Eq. (2) will be transformed into Eqs. (4) and (3) will be even more complex:

$$\mu_1(E) = \ln \frac{\mathrm{DM}_1\Delta_2(E, T_2, \mu_1(E))}{\mathrm{DM}_2\Delta_1(E, T_1, \mu_1(E))} \Big/ (T_2 - T_1), \tag{4}$$

where $\Delta_1(E, T_1, \mu_1(E))$ and $\Delta_2(E, T_2, \mu_1(E))$ are the buildup factors $[\Delta_2(E, T_2, \mu_1(E))/\Delta_1(E, T_1, \mu_1(E)) > 1]$ for the scattered photons, which are related to the beam energy E, material properties $\mu_1(E)$, and the thickness of the material. From Eq. (4), it is not possible to calculate $\mu_1(E)$ directly under the BBG condition. Because Eq. (3) cannot be solved, $\mu_1(E)$ under the continuous spectrum condition and the further derivation of Eq. (3) under the BBG condition is ignored.

In summary, using the channel ratio value to solve for $\mu_1(E)$, and then using $\mu_1(E)$ to solve for the beam energy E, the measurement error of E under the BBG condition will increase.

In practical application, through the narrow-spectrum series produced by an X-ray machine and a mono-energetic isotope radiation field, the relation between channel ratio value and beam energy can be obtained using the calibration method. The calibration method allows one to by-pass the process of Eqs. (2)–(4) to solve for $\mu_1(E)$ using the CRM, and the beam energy can be directly obtained using the LUT method.

3 Energy response correction using the channel ratio method

In practical application, it is essential to consider the consistency of aspects of the instrument, such as the filter material, the Si-PIN detector, and the circuit parameters. At the same time, the depletion layer of the Si-PIN detector and the surrounding material are not tissue equivalent. Calibration of the EPD under the standard radiation field can further simplify the mathematical calculation model. It is assumed that the counts per second (CPS) detected by

CH_1 and CH_2 are CT_1 and CT_2, and the CPS is linear with the dose rate. Assuming the dose rate at the position of the detector is D_s (μSv/h), the following relationship exists:

$$\begin{cases} CT_1 = a_1(E)D_s, \\ CT_2 = a_2(E)D_s. \end{cases} \quad (5)$$

The sensitivity coefficients $a_1(E)$ [CPS/(μSv/h)] and $a_2(E)$ [CPS/(μSv/h)] of the two-channel detectors are calibrated under the condition of energy E in the standard radiation field. In practical application, the sensitivity of the detector, the measuring range, and other technical parameters must also be considered. The composite material described in this paper is mainly composed of Al, Cu, and scintillation materials. A simplified model of Eq. (6) can be used to overcome the uncertain properties of materials such as size and density. There is no exact analytical formula for the function y in Eq. (6), which can be solved using the calibration method in a radiation protection standard laboratory.

$$E = y(CT_2/CT_1). \quad (6)$$

Equation (6) can be used to calculate the energy information of the radiation field using the LUT method.

Assuming $b_1(E) = 1/a_1(E)$ and $b_2(E) = 1/a_2(E)$, the accurate measurement of the personal dose rate equivalent can be accomplished using

$$\begin{cases} D_s = CT_1 b_1(E); \\ D_s = CT_2 b_2(E). \end{cases} \quad (7)$$

The conversion factors $b_1(E)$ and $b_2(E)$ can be calculated using the LUT method. After using Eq. (7) in the energy range between 48 keV and 1.25 MeV, the photon energy response of the EPD is corrected.

4 Characteristics of reference radiation field

A medium-energy reference radiation field is based on the narrow-spectrum series produced by an X-ray machine. A high-energy reference radiation field is based on $^{137}C_s$ and $^{60}C_o$ isotope radiation sources. The test conditions are summarized in Table 1, and the relevant standard values were obtained in a 1-L spherical ionization chamber (type 32002) at PTW Freiburg GmbH.

The narrow-spectrum series used in the research described in this paper mainly include N60, N80, N100, N120, N150, N200, and N250 [25, 26]. The energy spectrum is shown in Fig. 3 (normalized to the maximum counts).

It can be seen from Fig. 3 that the narrow-spectrum series have the characteristics of a continuous spectrum, but the attenuation law is similar to that of mono-energetic rays.

The testing setup in the standard laboratory is shown in Fig. 4. The prototype model of the EPD tested was Nt2000. The EPD was located in the front of the water phantom and the Si-PIN detector was coincident with the center of the radiation field.

5 Results and discussion

The counts per second (CPS) detected by the two-channel detectors are shown in Table 2. There were 10 measurements made in each energy condition, and the CPS values in Table 2 are the arithmetic means of the 10 measured values in each energy condition. It can be seen from the results presented in the table that the photon energy responses of the two-channel detectors are inconsistent in the energy range between 48 keV and 1.25 MeV.

The EPD uses a single-channel detector (CH_1) to obtain the counts-dose rate conversion factor $b_1(E)$ [(μSv/h)/CPS] (as shown in Fig. 5) under the different beam energy conditions in the standard laboratory. The standard deviation of the counts-dose rate conversion factors of all energy conditions are between 0.016 and 0.039, and the standard deviation at the kink point of 207.5 keV is 0.023. If the photon energy response of CH_1 is not corrected, the difference response from low energy to high energy can be up to approximately five times. This situation will seriously affect the accurate measurement of the personal dose equivalent for radiation field staff.

The plot shown in Fig. 6 was calculated in accordance with Eq. (2). Because the filter material, detector, and back-end circuit parameters may be inconsistent, the calculation results in Fig. 6 did not consider the density and thickness of the composite material. The standard deviation of the natural logarithm of the CT_1/CT_2 of all energy conditions is between 0.022 and 0.046, and the standard deviation at the kink point of 207.5 keV is 0.024. Under the $^{137}C_s$ and $^{60}C_o$ conditions, the CT_1/CT_2 values are 1.077 and 0.868, respectively. As a result, the natural logarithm of the CT_1/CT_2 is negative in the $^{60}C_o$ condition. The reason for the above phenomenon is that the influence of the scattered photons in matter is neglected in Eq. (2). Because the purpose of this article is to determine the relationship between the channel ratio value and the beam energy, as long as they have a one-to-one relationship, the above problems have no effect on practical application. It can be seen from the curve of Fig. 6 that the natural logarithm of the CT_1/CT_2 satisfies the monotone function characteristic in the energy range from 48 keV to 1.25 MeV, which

Table 1 Radiation qualities used in radiation protection

	Tube voltage (kV)	Tube current (mA)	Additional filtration (mm)				Half-value layer (HVL) for mm Cu	Distance (m)	Mean energy (keV)	Standard value (μSv/h)
			Al	Cu	Pb	Sn				
Narrow spectrum	60	1.5	4.0	0.61	/	/	0.24	3.0	47.9	1549
	80	2.3	4.0	1.95	/	/	0.58	3.0	65.0	1498
	100	4.3	4.0	4.70	/	/	1.10	3.0	83.1	1496
	120	3.6	4.0	4.17	/	1.03	1.68	3.0	100.0	1515
	150	0.6	4.0	0.65	/	2.11	2.33	3.0	117.7	1563
	200	1.1	4.0	1.98	1.14	1.47	3.95	3.0	164.0	1436
	250	0.8	4.0	/	1.98	2.95	5.15	3.0	207.5	1478
Isotope source	$^{137}C_s$						/	1.0	661.6	1148
	$^{60}C_o$						/	1.0	1250.0	7334

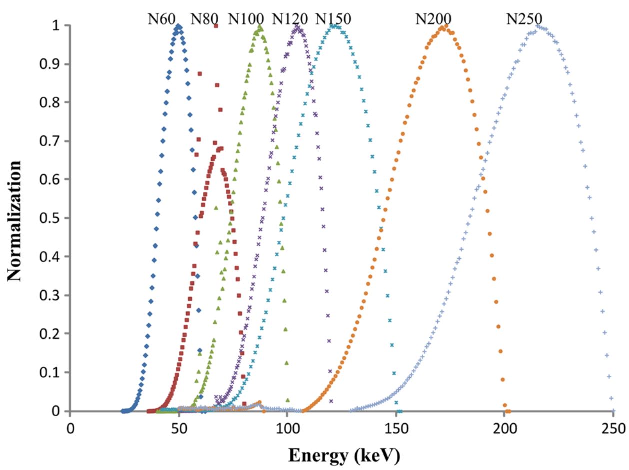

Fig. 3 (Color online) Characteristics of the narrow-spectrum series

further proves the feasibility of using the channel ratio value to identify the beam energy.

Figure 7 plots the discrete data points of the function y in Eq. (6). The standard deviation of the CT_2/CT_1 of all energy conditions is between 0.013 and 0.019, and the standard deviation at the kink point of 207.5 keV is 0.019. It can be seen from Fig. 7 that, although there is no linear or exponential relationship between the beam energy and the channel ratio value, there is a one-to-one relationship between them, which meets the requirement of Eq. (2). The relationship between the beam energy and the channel ratio value can be realized by polynomial fitting or by interpolation in the energy range between 48 keV and 1.25 MeV. Using the relation curve of Fig. 7, the beam energy can be directly identified by the channel ratio value.

Figure 8 shows the relationship between the channel ratio value (CT_2/CT_1) and the counts-dose rate conversion factor of CH_1. Owing to the change tendencies of the detector's conversion factor over the entire energy range being different, the conversion factors in the low- and high-energy regions can be fitted. It can be seen from Fig. 8 that the counts-dose rate conversion factor $[b_1(E)]$ of CH_1 can also be directly obtained from the channel ratio value (CT_2/CT_1).

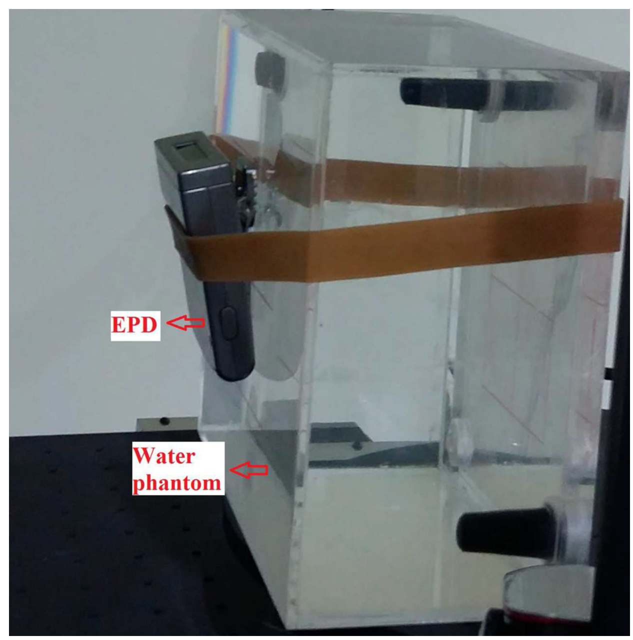

Fig. 4 (Color online) EPD field measurement setup in the standard laboratory

It can be seen from Figs. 6, 7 and 8 that the standard deviation exhibits no obvious differences between the kink point and the other points under the experimental conditions.

Table 2 Counts per second of CH_1 and CH_2

Mean energy (keV)	47.9	65.0	83.1	100.0	117.7	164.0	207.5	661.6	1250.0
Standard value (μSv/h)	1549	1498	1496	1515	1563	1436	1478	1148	7334
CT_1 (CPS)	2895	2703	2251	2153	2081	1849	1735	732	3305
CT_2 (CPS)	809	1032	1001	1084	1187	1278	1355	680	3808

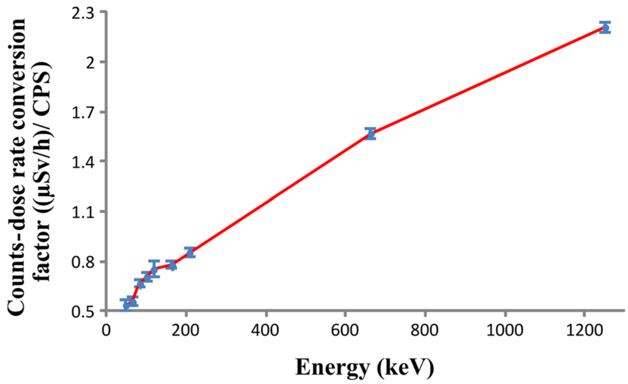

Fig. 5 (Color online) Counts-dose rate conversion factor of CH_1 as a function of photon energy

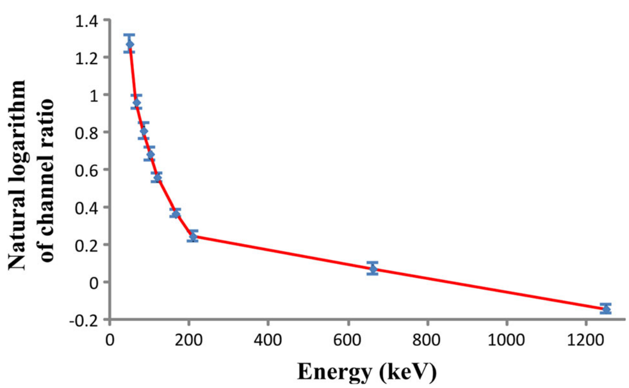

Fig. 6 (Color online) Natural logarithm of the channel ratio value (CT_1/CT_2) as a function of photon energy

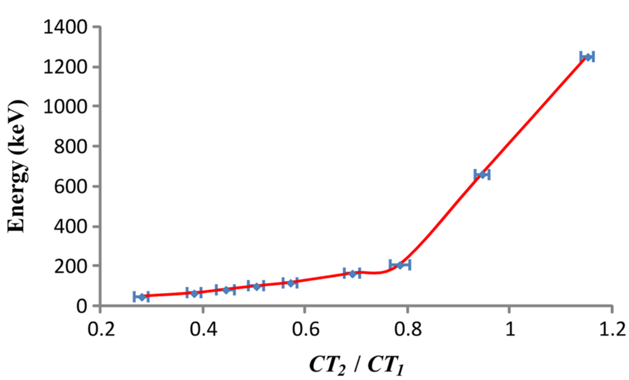

Fig. 7 (Color online) Photon energy as a function of the channel ratio value (CT_2/CT_1)

Table 3 presents the measurement results after the energy response correction of the EPD. Ten measurements were made for each condition. The measured values in

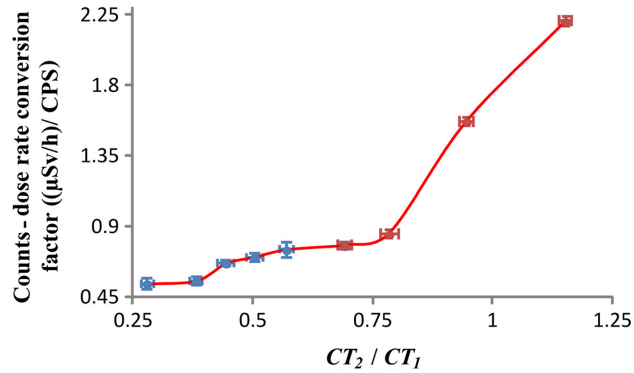

Fig. 8 (Color online) Counts-dose rate correction factor (CH_1) as a function of the channel ratio value (CT_2/CT_1)

Table 3 are the arithmetic mean of the ten values in each energy condition. The personal dose rate equivalent $H_p(10)$ parameters can be calculated using the CRM, and the measurement accuracy compared to the traditional single-channel method is significantly improved.

It can be seen from Fig. 9 that the photon energy response to $^{137}C_s$ using the CRM is similar to a horizontal line. The standard deviation of the corrected energy response to $^{137}C_s$ is between 0.016 and 0.040. The relative error of the personal dose rate equivalent is within $\pm 6.6\%$. The difference of the energy response to $^{137}C_s$ is within $\pm 6.0\%$, which fulfills the $\pm 30\%$ requirement of GB/T 13161-2003 and JJG 1009-2006.

6 Conclusion

In this paper, we described the use of composite screen detection technology, multichannel acquisition technology, and the CRM, by identifying the beam energy information, to achieve photon energy response correction for an EPD in the energy range from 48 keV to 1.25 MeV. At the same time, the principle and method of the photon energy response correction were derived, and the relevant features of the standard radiation field were described. The proposed method has the advantages of simple structure, easy implementation, low cost, low power consumption, and high measurement accuracy. The CRM was used to correct the photon energy response of the EPD, and the difference of the energy response to $^{137}C_s$ was almost constant within $\pm 6.0\%$, which fulfilled the energy response requirement of GB/T 13161-2003 and JJG 1009-2006. From the related

Table 3 Corrected measurement results using the CRM

Energy (keV)	47.9	65.0	83.1	100.0	117.7	164.0	207.5	661.6	1250.0
Standard value (μSv/h)	1549	1498	1496	1515	1563	1436	1478	1148	7334
Measured value (μSv/h)	1510	1478	1486	1530	1503	1465	1501	1140	6850
Relative error (%)	−2.52	−1.34	−0.67	0.99	−3.84	2.02	1.56	−0.70	−6.60
Relative response to $^{137}C_s$	0.98	0.99	1.00	1.02	0.97	1.03	1.02	1.00	0.94
Response difference to $^{137}C_s$ (%)	−1.83	−0.64	0.03	1.70	−0.32	2.74	2.27	0.00	−5.94

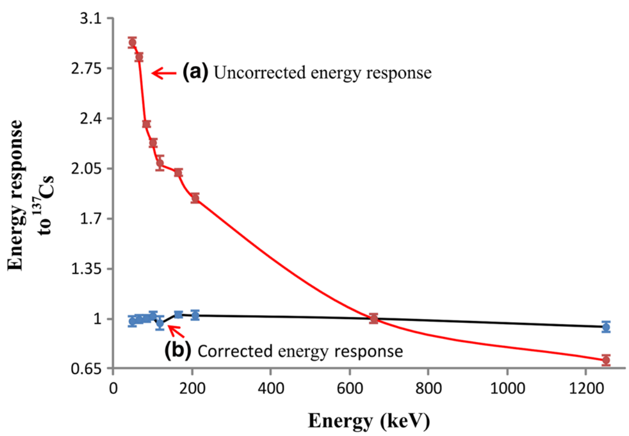

Fig. 9 (Color online) *a* Uncorrected energy response and *b* corrected energy response

test results, it was shown that the proposed method can realize the accurate measurement of the personal dose equivalent of radiation workers, and the method has practical application value in a personal dose monitoring system.

Although the channel ratio value and the beam energy have a one-to-one relationship, the relationship between them is not linear. The CRM is thus more suitable for personal dose equivalent measurement in mono-energetic conditions. When the EPD is used in a mixed radiation field, the measurement error of the personal dose equivalent will increase. In the future, it will be necessary to research the measurement method in a standard mixed radiation field.

References

1. L.A. Benevides, R.K. Piper, A. Romanyukha, A performance comparison of thermo fisher EPD-MK2 and TLD (LiF:Mg, Cu, P) as part of accreditation proficiency testing. Radiat. Meas. **71**, 183–186 (2014). doi:10.1016/j.radmeas.2014.03.019
2. J.G. Alves, Developments in standards and other guidance for individual monitoring. Radiat. Meas. **43**, 558–564 (2008). doi:10.1016/j.radmeas.2007.12.044
3. F. Wang, M.Y. Wang, F.S. Tian et al., Study on two-dimensional distribution of X-ray image based on improved Elman algorithm. Radiat. Meas. **77**, 1–4 (2015). doi:10.1016/j.radmeas.2015.03.012
4. J.F. Qian, T.Y. Shen, *Nuclear Radiation Dosimetry* (National Defense Industry Press, Beijing, 2009), pp. 199–278 **(in Chinese)**
5. Z. Li, X.G. Tuo, R. Shi et al., Analytic fitting and simulation methods for characteristic X-ray peaks from Si-PIN detector. Nucl. Sci. Tech. **24**, 060206 (2013). doi:10.13538/j.1001-8042/nst.2013.06.007
6. T. Ishikura, K. Aoyama, T. Fujimoto et al., Development of a small semiconductor detector using a printed circuit silicon-board for a personal dosemeter. Radiat. Meas. **43**, 546–549 (2008). doi:10.1016/j.radmeas.2008.01.009
7. H. Sato, O. Maida, T. Ito, Structure optimization of diamond personal dosimeters based on Monte Carlo simulations. Diam. Relat. Mater. **20**, 140–144 (2011). doi:10.1016/j.diamond.2010.11.015
8. J. Barthe, Electronic dosimeters based on solid state detectors. Nucl. Instrum. Methods Phys. Res. Sect. B **184**, 158–189 (2001). doi:10.1016/S0168-583X(01)00711-X
9. Z.G. Jiang, Y.G. Yuan, H.Y. Wang et al., Development of a spherical tissue equivalent proportional counter for neutron monitoring. Nucl. Sci. Tech. **26**, 060403 (2015). doi:10.13538/j.1001-8042/nst.26.060403
10. P. Sun, Y.C. Fu, J. Hu et al., Electron irradiation effects of radiochromic PCDA vesicle gel dosimeters. Nucl. Sci. Tech. **26**, 050301 (2015). doi:10.13538/j.1001-8042/nst.26.050301
11. C.R. Chen, S.H. Jiang, H.H. Tseng et al., Energy response and filter compensation of Si PIN photodiode for personal dosimetry application. IEEE Trans. Nucl. Sci. **40**, 857–862 (1993). doi:10.1109/23.256674
12. H.H. Tseng, H.F. Chang, Energy compensation characteristics of Cu and Sn on low cost Si photodiodes for γ(x) dosimetry applications. IEEE Trans. Nucl. Sci. **39**, 1523–1527 (1992). doi:10.1109/23.173237
13. F. Wang, M.Y. Wang, Y.F. Liu et al., Obtaining low energy dose with CMOS sensors. Nucl. Sci. Tech. **25**, 060401 (2014). doi:10.13538/j.1001-8042/nst.25.060401
14. C.M. Deng, Z.S. Liu, Z.Y. Zhang et al., The research of semiconductor detector test and circuit for the SDM2000 personal dosimeter. China Nucl. Sci. Technol. Rep. **2**, 122–132 (2004) **(in Chinese)**
15. H.Z. Dizaji, T. Kakavand, F.A. Davani, Spectrometry and dosimetry of fast neutrons using pin diode detectors. Nucl. Instrum. Methods Phys. Res. Sect. A. **741**, 84–87 (2014). doi:10.1016/j.nima.2013.12.018
16. J.H. Wu, Y.J. Xu, S.L. Liu et al., Energy spectrum measurement and dose rate estimation of natural neutrons in Tibet region. Nucl. Sci. Tech. **26**, 060202 (2015). doi:10.13538/j.1001-8042/nst.26.060202

17. M. Slapa, M. Traczyk, A new concept of dosimeter with silicon photodiodes. IEEE Trans. Nucl. Sci. **43**, 1855–1859 (1996). doi:10.1109/NSSMIC.1995.510394
18. W. Lee, G. Cho, H.D. Kim, A radiation monitoring system with capability of gamma imaging and estimation of exposure dose rate. IEEE Trans. Nucl. Sci. **49**, 1547–1551 (2002). doi:10.1109/TNS.2002.1039698
19. B.J. Lee, W. Lee, G. Cho et al., Solid-state personal dosimeter using dose conversion algorithm. Nucl. Instrum. Methods Phys. Res. Sect. A. **505**, 403–406 (2003). doi:10.1016/S0168-9002(03)01108-2
20. P. Huang, F. Fang, Y.D. Zhang et al., The detection technology of PIN silicon photodiode applied in the n $/\gamma$ Mixed radiation field. Nucl. Electron. Detect. Technol. **31**, 1341–1343 (2011). doi:10.3969/j.issn.0258-0934.2011.12.010 **(in Chinese)**
21. M. Jung, C. Teissier, P. Siffert, A proposal for fast neutron personal real time dosimetry in mixed n, γ fields. Nucl. Instrum. Methods Phys. Res. Sect. A **431**, 264–272 (1999). doi:10.1016/S0168-9002(99)00241-7
22. M.C. Chen, L.H. Tian, Mass thickness measurements for dual-component samples utilizing equivalent energy of X-rays. Nucl. Sci. Tech. **25**, 040202 (2014). doi:10.13538/j.1001-8042/nst.25.040202
23. H. Michael, An Investigation into Silicon PIN Diode Detectors for Dosimetry Applications. Master Thesis, University of Surrey (2010)
24. M.J. Berger, XCOM: Photon cross sections database, v3.1. National Institute of Standards and Technology (NIST), U.S.A. (2010). http://www.nist.gov/physlab/data/xcom/index.cfm. Accessed Aug 2015
25. J.X. Chen, Y.F. Li, S.L. Liu, *JJG 1009-2006, Direct Reading Individual Personal Dose Equivalent (rate) Monitor for X and Gamma Radiation* (General Administration of Quality Supervision, Inspection and Quarantine of the People's Republic of China, Beijing, 2006) **(in Chinese)**
26. Y. Liu, *GB/T 13161-2003, Direct Reading Personal Dose Equivalent (rate) Monitor for X, Gamma Radiation* (General Administration of Quality Supervision, Inspection and Quarantine of the People's Republic of China, Beijing, 2003) **(in Chinese)**